Available online at www.sciencedirect.com

ScienceDirect

Ceramics International 33 (2007) 1263–1268

CERAMICS INTERNATIONAL

www.elsevier.com/locate/ceramint

Phase transformation in cordierite gel synthesized by non-hydrolytic sol–gel route

I. Janković-Častvan *, S. Lazarević, D. Tanasković, A. Orlović, R. Petrović, Dj. Janaćković

Faculty of Technology and Metallurgy, University of Belgrade, Karnegijeva 4, 11120 Belgrade, Serbia

Received 22 March 2006; received in revised form 18 April 2006; accepted 6 May 2006

Abstract

Cordierite gel was synthesized by non-hydrolytic sol–gel route, starting from aluminum chloride, TEOS and magnesium chloride dissolved in absolute ethanol. Crystallization of μ-cordierite from gel at temperatures between 900 and 1000 °C was confirmed by differential thermal analyses, X-ray and FTIR spectroscopy. Higher calcination temperature resulted in the transformation of μ- to α-cordierite. The value of Avrami parameter $n = 2.23$ for the μ-cordierite crystallization indicates contribution of different simultaneous mechanisms: homogeneous nucleation and three-dimensional crystallite growth due to homogeneity of gel and surface crystallization due to submicron particles of the gel.

Keywords: A. Sol–gel processes; D. Cordierite; Phase transformation

1. Introduction

The sol–gel process is useful technique for processing a large number of technologically important glasses, glass–ceramics and crystalline ceramics, mainly because of its ability to generate stoichiometric materials of high purity with good control over particle size [1]. To avoid problems due to the different hydrolysis rates of alkoxides in hydrolytic sol–gel routes, non-hydrolytic sol–gel processes based on the direct condensation of the precursors in aprotic solvents, can be used. Non-hydrolytic sol–gel process [2–4] includes the reaction between alkoxides and halides of certain elements (Al, Si, Ti and others), or between halides and organic oxygen compounds (ethers, aldehydes, ketones and others). During the reaction breaking of O–R bonds occurs, causing the formation of oxygen bridges (–O–) and alkyl halides:

$$\equiv\mathrm{SiOR} + \mathrm{XSi}\equiv \;\rightarrow\; \equiv\mathrm{Si{-}O{-}Si}\equiv + \mathrm{RX}$$

$$2(\equiv\mathrm{SiX}) + \mathrm{ROR} \rightarrow \equiv\mathrm{Si{-}O{-}Si}\equiv + 2\mathrm{RX}$$

$$22(\equiv\mathrm{SiX}) + \mathrm{R'C} = \mathrm{O} \rightarrow \equiv\mathrm{Si{-}O{-}Si}\equiv + \mathrm{R'CX_2}$$

$$2\mathrm{Al(OR'')_3} + \mathrm{AlX_3} \rightarrow 2\mathrm{AlO_{3/2}} + 3\mathrm{R''X}$$

$$2\mathrm{AlX_3} + 3/2\mathrm{ROR} \rightarrow \mathrm{AlO_{3/2}} + 3\mathrm{RX}$$

$$2(\mathrm{X} = \mathrm{Cl, Br;\ R', R''} = \textit{iso}\text{-propil}, \textit{sec}\text{- or } \textit{tert}\text{- butyl group})$$

Many investigations are related to the synthesis and characterization of various gels and metal oxides by the non-hydrolytic route, such as Al_2O_3 [2,5–7], mullite [5,8,9], SiO_2 [4,6], TiO_2 [3], SiO_2–ZrO_2 [10], SiO_2–TiO_2 [10], ZrW_2O_8 [11], aluminum titanate [12], zirconium titanate [13].

Cordierite ($2MgO{\cdot}2Al_2O_3{\cdot}5SiO_2$) occurs in three polymorphous forms: hexagonal high-temperature form (α-cordierite or indialite), orthorhombic low-temperature form (β-cordierite) and metastable form (μ-cordierite). Due to its properties such as low thermal expansion coefficient, low dielectric constant, high specific resistivity and relatively high refractoriness [14] it is used in the manufacture of heating element supports, refractory ceramics for furnaces, oven-ware [15,16], insulating material in high-frequency electronics, as well as substrates for integrated circuits and electronic modules [17]. Special attention was paid to the application of cordierite as a catalyst support in high-temperature catalytic processes, especially in the conversion of the exhaust gases (CO, NO_x, hydrocarbons) from internal-combustion engines [18,19].

It is difficult to produce dense cordierite ceramics by the solid-state reaction without sintering aids, because of the narrow sintering range near the incongruent melting point of cordierite. These aids, on the other hand, increase the thermal expansion coefficient and dielectric constant. For that reason, recent studies on cordierite ceramics focused on the chemical

---

* Corresponding author.
E-mail address: nht@tmf.bg.ac.yu (I. Janković-Častvan).

doi:10.1016/j.ceramint.2006.05.003

synthesis of fine, reactive powders which can be sintered at lower temperatures, without sintering aids.

Studies on the sol–gel synthesis of cordierite [20–22] confirmed that from colloidal, triphasic gels, crystallization of spinel and cristobalite (or quartz) occurred, forming α-cordierite by reaction. From the monophasic, homogeneous gels crystallization of μ-cordierite occurs, transformed to α-cordierite at higher temperatures.

In earlier studies there are no data on the cordierite synthesis by the non-hydrolytic sol–gel route. The aim of this study was the synthesis of cordierite gel by non-hydrolytic sol–gel route, and investigation of the phase transformation during heat treatment of the gel.

2. Experimental procedure

2.1. Synthesis and characterization

For the synthesis of cordierite gel, the following compounds were used: tetraethyl orthosilicate—TEOS ($(C_2H_5O)_4Si$) (Fluka), magnesium chloride ($MgCl_2$) (Fluka), aluminum chloride ($AlCl_3$) (Fluka) and absolute alcohol (C_2H_5OH) (Hemos). Reactants were of p.a. grade.

The reactants were mixed in a stoichiometric ratio for cordierite (Mg:Al:Si = 2:4:5) in a glove box, and atmosphere of nitrogen. As a first step, 10.93 g of $AlCl_3$ was dissolved in 21.35 g of TEOS while intensive stirring. Then, 3.91 g of $MgCl_2$ was separately dissolved in 75 g of absolute alcohol, stirring vigorously. This solution was added stepwise to the solution of aluminum chloride and TEOS. The mixture obtained this way was heated in an autoclave at 150 °C for 3 h. The obtained gel was transparent, pale yellow. The gel was dried at 100 °C, in a flow of nitrogen, and calcined at temperature 650 °C for 2 h. White powder was then calcined, in an atmosphere of air, at different temperatures: 900, 1000, 1100, 1200, 1300 and 1350 °C for 2 h.

Differential thermal analysis (DTA) of the powder calcined at 650 °C was performed in N_2 on SDT Q600 instrument, up to the temperature of 1300 °C. The heating rate was 20 °C min^{-1} and Al_2O_3 was used as a standard.

Phase composition of the powders calcined at various temperatures was determined on the SIEMENS D500 diffractometer, with Cu Kα radiation in 2θ angle range from 5 to 60°, with a 0.02° step.

FTIR analysis of the specimens was determined on the MB BOMEM 100 HARTMANN and BRAUN spectrometer, within a wave number range from 400 to 1600 cm^{-1}. The specimens were prepared by the KBr method, in a mass ratio of specimen/KBr = 1:100.

The SEM analysis of the powders obtained by calcination of gel at 1000 °C was performed on the JEOL-T20. The powders were previously fumed with the Pd–Pt alloy.

2.2. Determination of the kinetics of the phase transformation

The phase transformation kinetics was studied on the gel previously calcined at temperature 650 °C. The kinetic parameters were determined by the differential thermal analysis, under non-isothermal conditions, up to 1100 °C at heating rates of 10, 15, 20 and 24 °C min^{-1}. The sample mass, in all cases, was 170 mg.

Table 1
Values of *n* for different growth and nucleation conditions

Growth and nucleation conditions	Diffusion	Interface
Constant nucleation rate		
Three-dimensional growth	5/2	4
Two-dimensional growth	3/2	3
One-dimensional growth	1/2	2
Constant particle number		
Three-dimensional growth	3/2	3
Two-dimensional growth	2/2	2
One-dimensional growth	1/2	1
Surface nucleation	1/2	1

The Avrami parameter, *n*, indicating a mechanism of nucleation and growth mechanism, was determined using Ozawa method [23] expressed by the following relation:

$$\log(-\ln(1-\alpha)) = n\log(K(T-T_0)) - n\log Q \quad (1)$$

where α is the degree of transformation, Q the heating rate, T_0 the initial temperature, T the temperature recorded after time t, K is a constant and n is the Avrami parameter.

The plot of $\log(-\ln(1-\alpha))$ versus $\log Q$, at the chosen temperature, results in a straight line and the value of n can be determined from its slope. The value of α was determined from a series of DTA curves obtained at various heating rates, from the following relation:

$$\alpha = \frac{S}{S_0} \quad (2)$$

where S is the partial peak area from the beginning of peak to a chosen temperature and S_0 is the total peak area. Data on the early and final stages of transformations were not taken into account, due to some limitations related to these stages [24] and to application of most of the kinetic equations. Therefore, the temperatures for which the degree of transformation, α, at all heating rates lies in the range 0.2–0.7 were selected.

Values of parameter n, for different growth and nucleation conditions [25], are given in Table 1.

3. Results and discussion

3.1. Phase transformations during thermal treatment of the gel

Fig. 1 presents the differential thermal analysis curve for the calcined gel at the heating rate of 20 °C min^{-1}. First exothermal peak at temperature 967 °C can be assigned to the crystallization of μ-cordierite from the amorphous phase, while second exothermal peak at 1202 °C probably corresponds to the μ → α-cordierite transformation [21,26,27]. There is one more exothermal peak at 1257 °C. In order to determine which processes or reactions really corresponding to the mentioned

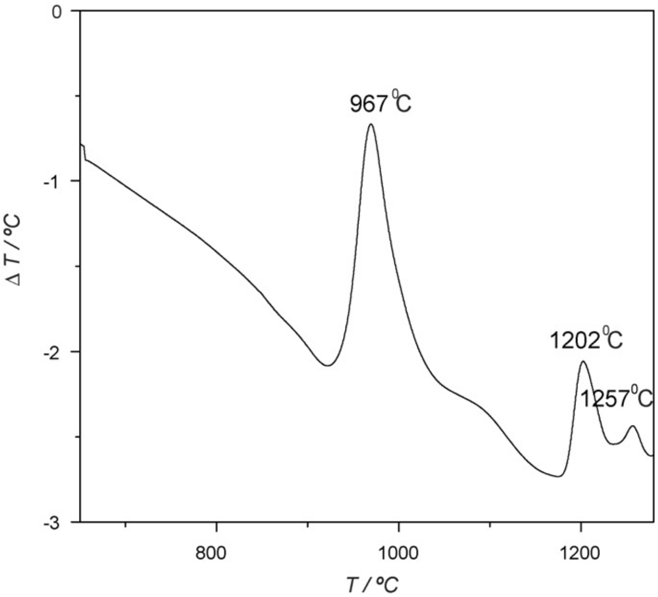

Fig. 1. DTA curve of the cordierite gel calcined at temperature 650 °C for 2 h (heating rate 20 °C min^{-1}).

exothermal peaks, the gel was calcined at temperatures 900, 1000, 1100, 1200, 1300 and 1350 °C.

Fig. 2 presents the diffractograms of the powders obtained by calcining cordierite gel at temperatures 900, 1000, 1100, 1200, 1300 and 1350 °C for 2 h.

An intense and sharp peak corresponding to μ-cordierite has been observed in the diffractogram of the powders obtained by calcining cordierite gel at temperatures 900, 1000, 1100 and 1200 °C, as well as somewhat weaker peaks corresponding to spinel [21]. This confirms that peak at 967 °C on DTA curve is a consequence of the crystallization of μ-cordierite. With the increasing of calcining temperature from 900 to 1200 °C, the intensity of peaks corresponding to μ-cordierite slightly change, while the intensity of peaks assigned to spinel is increasing. The diffractograms of the powders obtained by calcination at temperatures 1300 and 1350 °C are very similar, and fully corresponding to α-cordierite. On the basis of these diffractograms it can be concluded that the transformation from μ- to α-cordierite occurs within a temperature interval from 1200 to 1300 °C. Furthermore, it is obvious that at the same temperature interval, α-cordierite is formed also by the reaction [28] between spinel and amorphous SiO_2 since diffractogram of the powder calcined at 1300 °C indicates the disappearance of peaks associated with spinel. The results of X-ray analyses confirm that first exothermal peak at DTA curve corresponds to the crystallization of μ-cordierite and second exothermic peak corresponds to $\mu \rightarrow \alpha$-cordierite transformation. Third exothermal peak obviously corresponds to the formation of α-cordierite by the reaction of amorphous SiO_2 and spinel. Spinel crystalization ocurrs at the same temperature interval as well as the crystallization of μ-cordierite.

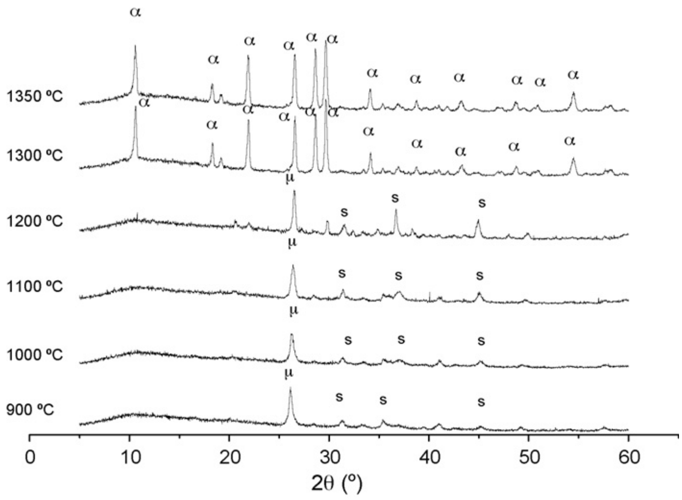

Fig. 2. Diffractograms of the powders obtained by calcining gel at temperatures 900, 1000, 1100, 1200, 1300 and 1350 °C for 2 h (μ: μ-cordierite; α: α-cordierite; S: spinel).

The results of FTIR spectroscopy of the powders obtained by calcining cordierite gel at temperatures 900, 1000, 1100, 1200, 1300 and 1350 °C are presented in Fig. 3.

In the FTIR spectrum of powder, obtained by calcination of the gel at 900 °C, bands characteristic for μ-cordierite [29] at ~450, ~940 and ~1100 cm^{-1}, and band characteristic for spinel [30,31] at ~560 cm^{-1}, can be observed. These bands are more intensive in FTIR spectrum of the powder, obtained by calcination of the gel at temperatures 1000 and 1100 °C. In addition, the presence of new bands at ~700 and ~790 cm^{-1} has been observed, characteristic of spinel [30,31]. The FTIR spectrum of the powder obtained by calcining the gel at temperature 1200 °C indicates the beginning of transformation

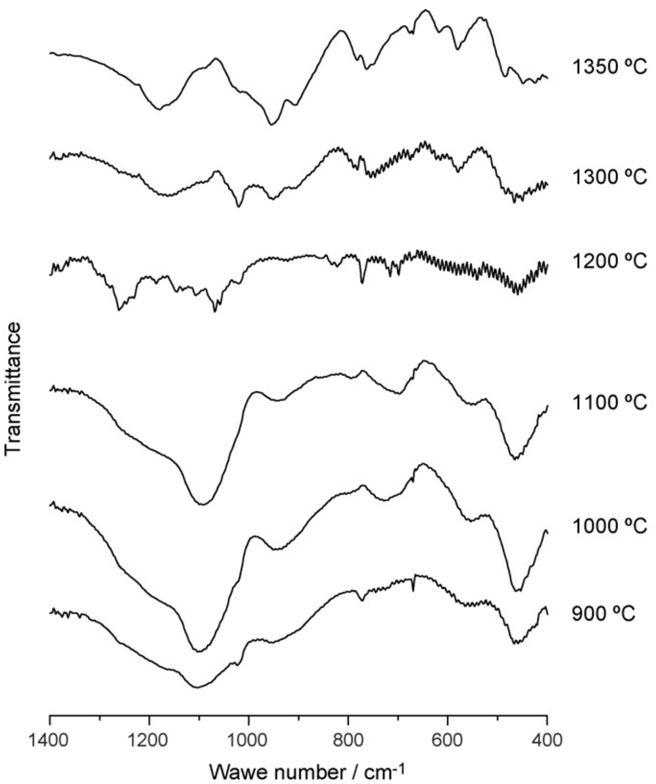

Fig. 3. FTIR spectra of the powders obtained by calcining gel at temperatures 900, 1000, 1100, 1200, 1300 and 1350 °C for 2 h.

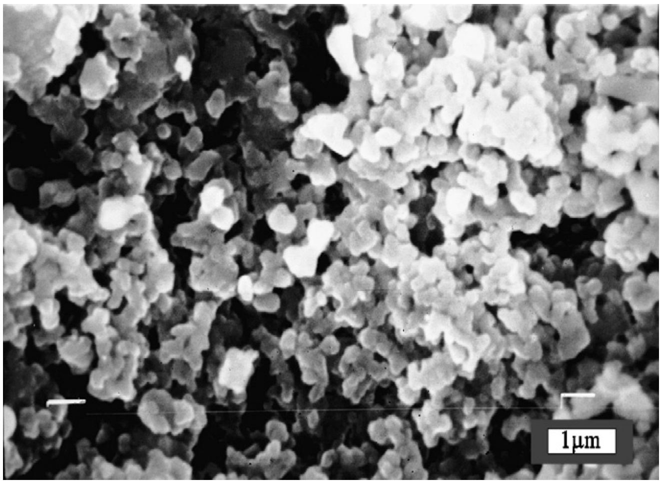

Fig. 4. SEM micrograph of the cordierite powder obtained by gel calcination at temperature 1000 °C for 2 h.

of μ-cordierite to α-cordierite. Despite the fact that the diffractogram of this powder indicates the presence of μ-cordierite and spinel, FTIR spectrum shows appearance of bands splitting typical for μ-cordierite, as well as the incipient formation of the bands corresponding to α-cordierite [29]. In the FTIR spectra of the powders obtained by calcining cordierite gel at temperatures 1300 and 1350 °C the following bands distinctive for α-cordierite were observed: band at 470 and 580 cm^{-1} corresponds to Si–O bond vibrations and MgO_6 octahedra, respectively, while band at 770 cm^{-1} is associated to a six-membered ring of tetrahedra within the cordierite structure. Two more bands at 950 and 1180 cm^{-1} are related to vibrations of Al–O bond within a tetrahedron [29]. These bands are more intensive in the spectrum of the powder calcined at 1350 °C, indicating a higher degree of crystallinity. The results of the FTIR spectroscopy confirm the conclusions about the phase composition, drawn on the basis of the X-ray analysis.

Micrograph of the cordierite powder obtained by calcining gel at 1000 °C is presented in Fig. 4. It has been observed, from this figure, that the particles are spherical, with a relatively uniform size distribution and mainly within a range of 200–300 nm.

3.2. Crystallization kinetics of μ-cordierite

DTA curves of the powder obtained by calcinations of cordierite gel at temperature 650 °C, at the heating rates of 10, 15, 20 and 24 °C min^{-1} are presented in Fig. 5.

An exothermic peak, observed in the DTA curve, shifts towards higher temperatures, as the heating rate increases. According to the results of both, the X-ray and FTIR analyses, this exothermic peak corresponds to the crystallization of μ-cordierite.

From the dependence $\log(-\ln(1-\alpha))$ versus $\log Q$, at 955 °C, illustrated in Fig. 6, for a peak corresponding to crystallization of μ-cordierite, value of the Avrami parameter n can be obtained by the Ozawa method (Eq. (1)).

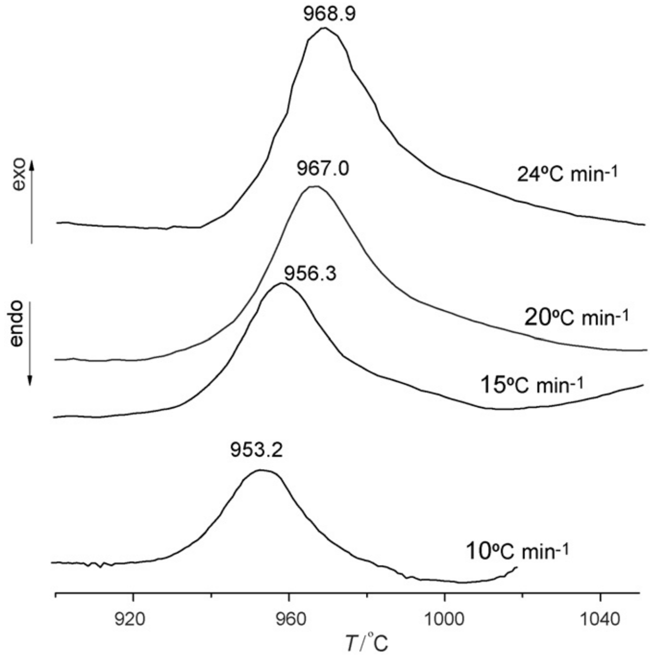

Fig. 5. DTA curves of the cordierite gel calcined at temperature 650 °C for 2 h (heating rates 10, 15, 20 and 24 °C min^{-1}).

The value of parameter n, from the slope of the straight line in Fig. 6, was 2.28. The values of the parameter n at temperatures of 955, 958, 960, 962 and 965 °C, determined in the same way, are presented in Table 2. The mean value of the Avrami parameter n for the crystallization of μ-cordierite was 2.23.

On the basis of Avrami parameter value, dominant mechanism of crystallization of μ-cordierite cannot be suggested. If the dominant mechanism is crystallization from homogenous monophasic gels, with constant nucleation rate

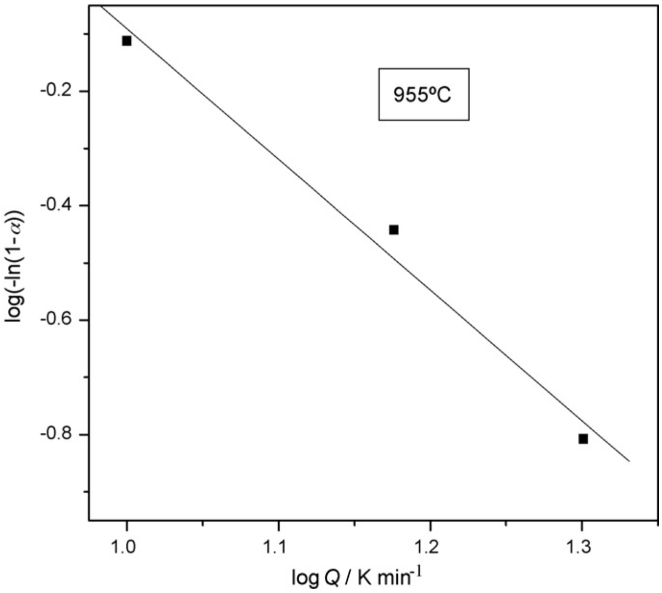

Fig. 6. Dependence $\log(-\ln(1-\alpha))$ versus $\log Q$ at the temperature of 955 °C for the peak corresponding to μ-cordierite crystallisation.

Table 2
Values of the Avrami parameter *n* at various temperatures

T (°C)	*n*
955	2.28
958	2.31
960	2.10
962	2.42
965	2.07

and three-dimensional growth, the value of parameter n will be 4. Petrovic et al. investigated [21,31] the kinetics of μ-cordierite crystallization from alkoxy-derived cordierite gel, obtained by hydrolytic sol–gel process, and obtained the theoretically expected value for the homogeneous gels, $n = 4$. Lim and Jang [22] also investigated kinetics of μ-cordierite from the monophasic gels of cordierite composition, by the isothermal process. Expected value $n = 3$ has been found for a gel with the addition of μ-cordierite crystal seeds, and $n = 2.7$–3.1 without the addition crystal seeds, differing considerably from a theoretically expected value $n = 4$ for crystallization from homogenous monophasic gels. These authors assumed that in this case, a surface nucleation and two-dimensional growth occur.

Value of $n = 2.23$, obtained in this study, is considerably different from the theoretically expected value of $n = 4$ for homogenous gels. Considering the results of X-ray, FTIR and SEM analyses, it can be assumed that different mechanisms of μ-cordierite crystallization influenced the value of parameter n: homogenous nucleation and three-dimensional crystallite growth ($n = 4$) as well as surface nucleation and crystallization ($n = 1$). Micrograph of the cordierite powder, obtained by calcining gel at 1000 °C, shows particles of submicron size, therefore a significant contribution of surface nucleation and crystallization can be expected. Also, the value of parameter n for crystallization of μ-cordierite can be influenced by crystallization of spinel which takes place in the same temperature interval. From this observations, it can be suggested that the value of parameter $n = 2.23$ for the crystallization of μ-cordierite is the result of various mechanisms contribution.

4. Conclusion

In summary, the present work demonstrates that cordierite can be synthesized using a non-hydrolytic sol–gel approach, by the reaction of metal chlorides and alkoxide precursor. The crystallization of μ-cordierite induced by heat treatment of the gel proved its homogeneity, but the appearance of spinel crystallization at the same temperature indicates certain gel inhomogeneity. In the temperature interval from 1200 to 1300 °C the α-cordierite was formed by the transformation of μ-cordierite, and also by the reaction of spinel and amorphous SiO_2. This way, the heat treatment of the gel at 1300 °C yielded pure α-cordierite.

The value of Avrami parameter $n = 2.23$, for the μ-cordierite crystallization, determinated by the Ozawa method, indicates contribution of different simultaneous mechanisms: homogeneous nucleation and three-dimensional crystallite growth due to homogeneity of gel and surface nucleation and crystallization due to submicron particles of the gel.

Acknowledgments

The financial support through the Ministry of Science and Environmental Protection, Republic of Serbia, Project No. 142070B, is gratefully acknowledged.

References

[1] R. Petrović, Dj. Janacković, B. Božović, S. Zec, Lj. Kostić-Gvozdenović, Densification and crystallization behaviour of colloidal cordierite-type gels, J. Serb. Chem. Soc. 66 (2001) 335.
[2] S. Acosta, R.J.P. Curriu, D. Leclercq, L. Lefevre, P.H. Mutin, A. Vioux, Preparation of alumina gels by a non-hydrolytic sol–gel processing method, J. Non-Cryst. Solids 170 (1994) 234.
[3] P. Arnal, R.J.P. Curriu, D. Leclercq, P.H. Mutin, A. Vioux, Preparation of anatase, brookite and rutile at low temperature by non-hydrolytic sol–gel methods, J. Mater. Chem. 6 (1996) 1925.
[4] R.J.P. Curriu, D. Leclercq, L. Lefevre, P.H. Mutin, A. Vioux, Preparation of monolithic gels from silicon halides by a non-hydrolytic sol–gel process, J. Non-Cryst. Solids 146 (1992) 301.
[5] S. Acosta, R. Corriu, D. Leclercq, P.H. Mutin, A. Vioux, Novel non-hydrolytic sol–gel route to metal oxides, J. Sol–Gel Sci. Technol. 2 (1994) 25.
[6] J.N. Hay, H.M. Raval, Preparation of inorganic oxides via a non-hydrolytic sol–gel route, J. Sol–Gel Sci. Technol. 13 (1998) 109.
[7] G.S. Grader, Y. de Hazan, Y. Cohen, D. Bravo-Zhivotovskii, Effect of aging on nonhydrolytic alumina xerogels, J. Sol–Gel Sci. Technol. 10 (1997) 5.
[8] Dj. Janacković, A. Orlović, D. Skala, S. Drmanić, Lj. Kostić-Gvozdenović, V. Jokanović, D. Uskoković, Synthesis of nanostructured mullite from xerogel and aerogel obtained by non-hydrolytic sol–gel method, Nanostruct. Mater. 12 (1999) 147.
[9] S. Acosta, R.J.P. Corriu, D. Leclercq, P.H. Mutin, A. Vioux, Monophasic pre-mullite gels prepared by a non-hydrolytic process, Mater. Res. Soc. Symp. Proc. 346 (1994) 345.
[10] M. Andrianainarivelo, R. Corriu, D. Leclercq, P.H. Mutin, A. Vioux, Mixed oxides SiO_2–ZrO_2 and SiO_2–TiO_2 by a non-hydrolytic sol–gel route, J. Mater. Chem. 6 (1996) 1665.
[11] A.P. Wilkinson, C. Lind, S. Pattanaik, A new polymorh of ZrW_2O_8 prepared using nonhydrolytic sol–gel chemistry, Chem. Mater. 11 (1999) 101.
[12] M. Andrianainarivelo, R.J.P. Corriu, D. Leclercq, P.H. Mutin, A. Vioux, Non-hydrolytic sol–gel process: aluminium titanate gels, Chem. Mater. 9 (1997) 1098.
[13] M. Andrianainarivelo, R.J.P. Corriu, D. Leclercq, P.H. Mutin, A. Vioux, Non-hydrolytic sol–gel process: zirconium titanate gels, J. Mater. Chem. 7 (1997) 279.
[14] P. Predecki, J. Haas, J. Faber Jr., J.L. Hitterman, Structural aspects of the lattice thermal expansion of hexagonal cordierite, J. Am. Ceram. Soc. 70 (1987) 175.
[15] M. Tecilazić-Stevanović, T. Janaćković, Lj. Kostić-Gvozdenović, R. Ćirjaković, Dependance of the properties of cordierite-mullite ceramics on synthesis conditions, Ind. Ceram. 13 (1993) 31.
[16] Lj. Kostić-Gvozdenović, T. Janaćković, M. Tecilazić-Stevanović, B. Todorović, Glazes for cordierite ceramics, Ind. Ceram. 13 (1993) 11.
[17] J.C. Bernier, sol–gel processing for the synthesis of powders for dielectrics, Powder Metall. Int. 18 (1986) 164.
[18] A. Yamuna, R. Johnson, Y.R. Mahajan, M. Lalithambika, Kaolin based cordierite for pollution control, J. Eur. Ceram. Soc. 24 (2004) 65.
[19] L. Li, J. Chen, S. Zhang, N. Guan, M. Richter, R. Eckelt, R. Fricke, Study on metal–MFI/cordierite as promising catalysts for selective catalytic

reduction of nitric oxide by propane in excess oxygen, J. Catal. 228 (2004) 12.

[20] A.M. Kazakos, S. Komarneni, R. Roy, Sol–gel processing of cordierite: effect of seeding and optimization of heat treatment, J. Mater. Res. 5 (1990) 1095.

[21] R. Petrović, Dj. Janaćković, S. Zec, S. Drmanić, Lj. Kostić-Gvozdenović, Crystallization behavior of alkoxy-derived cordierite gels, J. Sol–Gel Sci. Technol. 28 (2003) 111.

[22] B.C. Lim, H.M. Jang, Crystallization kinetics and phase transformation characteristics in seeded monophasic cordierite gel, J. Mater. Res. 6 (1991) 2427.

[23] H. Yinnon, D.R. Uhlmann, Applications of thermoanalytical techniques to the study of crystallization kinetics in glass-forming liquids, Part I. Theory, J. Non-Cryst. Solids 54 (1983) 253.

[24] I.W. Donald, The crystallization kinetics of a glass based on the cordierite composition studied by DTA and DSC, J. Mater. Sci. 30 (1995) 904.

[25] K. Matusita, S. Sakka, Kinetic study on crystallization of glass by differential scanning calorimetry, Phys. Chem. Glasses 20 (1979) 2081.

[26] Dj. Janackovic, V. Jokanovic, Lj. Kostic-Gvozdenovic, S. Zec, D. Uskoković, Synthesis and formation mechanism of submicrometre spherical cordierite powders by ultrasonic spray pyrolysis, J. Mater. Sci. 32 (1997) 163.

[27] P.N. Kumta, R.E. Hackenbery, P. McMichael, W.C. Johnson, Solution sol–gel synthesis of cordierite xerogels, aerogels and thin films, Mater. Lett. 20 (1994) 355.

[28] M.A. Einarsurd, S. Pedersen, E. Larsen, T. Grande, Characterization and sintering of gels in the system MgO-Al_2O_3-SiO_2, J. Eur. Ceram. Soc. 19 (1999) 389.

[29] H. Suzuki, K. Ota, H. Saito, Preparation of cordierite ceramics from metal alkoxides (part 1): preparation and characterization of the powder, Yogyo-Kyokai-Shi (J. Ceram. Soc. Jpn.) 95 (1987) 163.

[30] R.A. Nyquist, R.O. Kagel, Infrared Spectra of Inorganic Compounds, Academic Press, New York, 1971, p. 37, 116, 188.

[31] R. Petrović, Dj. Janaćković, S. Zec, S. Drmanić, Lj. Kostić-Gvozdenović, Phase-transformation kinetics in triphasic cordierite gel, J. Mater. Res. 16 (2001) 451.